RESEARCH ARTICLE

Polyelectrolyte gelatin-chitosan hydrogel optimized for 3D bioprinting in skin tissue engineering

Wei Long Ng[1,2], Wai Yee Yeong[1*] and May Win Naing[2]

[1] Singapore Centre for 3D Printing (SC3DP), School of Mechanical and Aerospace Engineering, Nanyang Technological University (NTU), 50 Nanyang Avenue, Singapore 639798, Singapore

[2] Singapore Institute of Manufacturing Technology (SIMTech), Agency for Science, Technology and Research, 71 Nanyang Drive, Singapore 638075, Singapore

Abstract: Bioprinting is a promising automated platform that enables the simultaneous deposition of multiple types of cells and biomaterials to fabricate complex three-dimensional (3D) tissue constructs. Collagen-based biomaterial used in most of the previous works on skin bioprinting has poor printability and long crosslinking time. This posed an immense challenge to create 3D constructs with pre-determined shape and configuration at high throughput. Recently, the use of chitosan for wound healing applications has attracted huge attention due to its attractive traits such as its antimicrobial properties and ability to trigger hemostasis. In this paper, we optimized polyelectrolyte gelatin-chitosan hydrogel for 3D bioprinting. Modification to the chitosan was carried out via the oppositely charged functional groups from chitosan and gelatin at a specific pH of ~pH 6.5 to form polyelectrolyte complexes. The polyelectrolyte hydrogels were evaluated in terms of physical interactions within polymer blend, rheological properties (viscosities, storage and loss modulus), printing resolution at varying pressures and feed rates and biocompatibility. The polyelectrolyte gelatin-chitosan hydrogels formulated in this work was optimized for 3D bioprinting at room temperature to achieve high shape fidelity of the printed 3D constructs and good biocompatibility with fibroblast skin cells.

Keywords: 3D printing, bioprinting, rapid prototyping, additive manufacturing, skin tissue engineering

*Correspondence to: Wai Yee Yeong, Singapore Centre for 3D Printing (SC3DP), School of Mechanical and Aerospace Engineering, Nanyang Technological University (NTU), 50 Nanyang Avenue, Singapore 639798, Singapore; Email: wyyeong@ntu.edu.sg

Received: October 22, 2015; **Accepted:** December 17, 2015; **Published Online:** December 29, 2015

Citation: Ng W L, Yeong W Y and Naing M W, 2016, Polyelectrolyte gelatin-chitosan hydrogel optimized for 3D bioprinting in skin tissue engineering. *International Journal of Bioprinting*, vol.2(1): 53–62. http://dx.doi.org/10.18063/IJB.2016.01.009

1. Introduction

Tissue engineering has emerged as a multi-disciplinary field that involves clinicians, scientists and engineers to create anatomically relevant tissue constructs that alleviate the shortage of donor tissues/organs[1]. Despite major advancements in the field of tissue engineering, simple cell seeding over pre-formed polymeric scaffolds is not sufficient to fully replicate the sophisticated cell-matrix interactions within the native tissues[2]. The heterogeneity in extracellular matrix (ECM) composition within both epidermal and dermal regions of the skin plays numerous roles ranging from regulation of cellular proliferation to manipulation of stem cell fate. Bioprinting, which is an emerging technology, can be defined as "the use of 3D printing technology that incorporates viable living cells with biomaterials to fabricate sophisticated tissues/organs"[3]. The bioprinting technology not only enables the simultaneous deposition of different biomaterials and multiple cell types, but also provides flexibility in the design and fabrication of customizable patient-specific tissue-engineered constructs[4], demonstrating great potential for fabrica-

tion of complex 3D multicellular tissue constructs.

Despite being in its stage of infancy, bioprinting has already demonstrated great potential for fabrication of multi-layered skin[5–7], cartilage[8,9] and liver constructs[10]. It was highly anticipated that production of less-sophisticated human tissues/organs such as skin would be a reality in the near future[3]. Some current works on bioprinting of skin constructs include fabrication of hydrogel constructs consisting of different skin cells (keratinocytes and fibroblasts)[5,6] and *in-situ* printing of skin cells and biomaterials directly over the wound site[11]. Contrary to the common misconception that skin is a relatively simple 2D tissue, the thin layer of human skin has a unique pattern created by the natural compartmentalization of different types of skin cells that are positioned relative to each other at high degree of specificity[12]. This specific arrangement of skin cells is essential for cell-cell interactions that initiate autocrine and paracrine signaling within the native human skin[13].

As skin cells (fibroblasts) are capable of producing their own ECM proteins, the bio-inks serve as temporary 3D templates to guide the tissue morphogenesis. Collagen type I, the most abundant ECM protein in human skin, is widely used for bioprinting of skin constructs. Most of the biomaterials used in those studies[5,6,14–16] were mainly collagen-based, which has relatively poor printability. Lee *et al.* printed layers of collagen to create a 3D bioprinted collagen construct with stacking height of 1.2 mm[5]. Another work demonstrated printing of multi-layered cell-laden collagen constructs on non-planar surface using nebulized crosslinking reagent[15]. Only planar sandwich constructs were fabricated using the valve-based technique due to the slow pH-dependent crosslinking of collagen prior to printing of subsequent layers. Koch *et al.* printed layers of encapsulated keratinocytes and fibroblasts onto a decellularized dermal matrix sheet via laser-based method[6]. The printed construct comprised high number of keratinocytes and fibroblasts (different from representative cellular density within native human skin) and there is no variation in the extracellular matrix density across the depth of printed structure[17].

Progress in bioprinting of skin is severely hindered due to limited choices of printable biomaterials. Over the recent years, the attractive traits of chitosan polymer have gained huge attention for wound healing applications[18–20]. Chitosan is a linear polysaccharide of D-glucosamine and *N*-acetyl-D-glucosamine, which can be prepared by the *N*-deacetylation of insoluble chitin in the presence of alkaline solution[21]. In the presence of lysozymes, chitosan undergoes *in vivo* degradation via enzymatic hydrolysis to form by-product, glucosamine, which does not pose any toxicity[22]. Furthermore, chitosan triggers hemostasis and accelerates tissue regeneration due to the migration of inflammatory cells and activation of fibroblasts that produce multiple cytokines[23]. Notably, chitosan-based biomaterials have antimicrobial properties which can help to reduce the incidence of sepsis[24]. Chitosan powders are generally soluble at acidic pH and the amine groups in chitosan are protonated at pH lower than 6 to confer the poly-cationic behavior to chitosan. With increasing pH, the amine groups become deprotonated to form insoluble chitosan polymer. This soluble-insoluble transition occurs at its pK_a value around pH 6–6.5, which is dependent on degree of *N*-deacetylation and molecular weight[25]. Despite its attractive properties, chitosan alone has poor printability[26,27] and further modifications are required to increase the printability of chitosan-based hydrogels.

Gelatin, which is commonly used for biomedical applications, exhibits negative charges when the pH of medium is above its isoelectric point (pH_{iso} = 4.7)[28]. As such, interactions between the positively charged ammonium ions from chitosan react with carboxylate groups from the ampholytic gelatin result in the formation of a polyelectrolyte complex. Prior works on polyelectrolyte gelatin-chitosan scaffolds/films[29–32] have demonstrated great potential for skin tissue engineering applications. The polyelectrolyte gelatin-chitosan hydrogel did not experience significant contraction in the *in-vitro* cell culture test over 4 weeks[32] and also demonstrated potential antimicrobial activity[33]. An *in-vivo* study over a period of 16 weeks revealed that the chitosan/gelatin hydrogel was efficient in inducing fibrin formation and vascularization at the implant-host interface[34]. The polyelectrolyte gelatin-chitosan scaffolds are commonly prepared via freeze-drying[29,31,32] or solvent-casting approaches[29,30].

In this paper, gelatin was modified with chitosan to form polyelectrolyte gelatin-chitosan (PGC) hydrogels to demonstrate its potential for bioprinting applications. The interactions between the chitosan and gelatin within the polyelectrolyte complex were evaluated, followed by rheological characterization of the PGC hydrogels at varying shear rates and temperatures. Next, different combinations of printing pressures and feed rates were utilized for different PGC hydrogels to

determine the highest possible printing resolution and printing accuracy at room temperature. Lastly, biocompatibility tests were conducted to evaluate the potential use of PGC hydrogels for bioprinting of skin constructs. These outcomes will provide valuable insights into development of printable hydrogels for bioprinting of 3D tissue constructs.

2. Materials and Methods

2.1 Materials and Cells

Chitosan (low molecular weight, 75–85% deacetylation) and gelatin (porcine skin, Type A) powders were obtained from (Sigma Aldrich, Singapore). Other reagents like acetic acid, sodium hydroxide (NaOH) and phosphate buffered saline (PBS) solution (pH 7.4 at 0.01 M) were sterile-filtered before use. Neonatal human foreskin fibroblasts (HFF-1 from ATCC® SCRC-1041™) were used in this study. The cell line was cultured in a HERAcell 150i cell incubator (Thermo Scientific) at 37°C in 5% CO_2 using ATCC-formulated Dulbecco's Modified Eagle's Medium (DMEM) supplemented with 15% fetal bovine serum (HyClone™ from GE Healthcare). Culture media was changed every 3 days and the cells were routinely passaged in tissue culture flasks (cells were not used after Passage 6). The adherent HFF-1 cells were harvested using 0.25% trypsin/ethylenediaminetetraacetic acid (EDTA) (Invitrogen) at 90% confluency.

2.2 Synthesis of Polyelectrolyte Gelatin-chitosan Hydrogels

Modification of chitosan was carried out via the addition of gelatin to create a polyelectrolyte gelatin-chitosan hydrogel[30]. 2.5% w/v chitosan was dissolved in acetic acid and mechanically agitated for three hours to obtain a homogeneous gel. Varying concentration of gelatin solutions (2.5%, 5% and 7.5% w/v) were dissolved in sterile PBS solution and stirred at 40°C for complete dissolution of gelatin powder. The gelatin solution of varying concentration was then added separately to the chitosan gel at a pH greater than 4.7 to initiate the formation of polyelectrolyte complex between the positively-charged chitosan and negatively charged gelatin and they were designated hereafter as 2.5%, 5% and 7.5% PGC respectively. Equal volume of gelatin solution was added to the chitosan gel in a drop-wise manner under constant mechanical agitation, followed by subsequent addition of NaOH solution to the gelatin-chitosan polymer blend in a drop-wise manner till the pH of the mixture reaches ~ 6.5 to initiate the pH-dependent crosslinking using a pH meter (HM Digital. Inc.).

2.3 FTIR Characterization

The interactions between chitosan and gelatin within the polymer blend were investigated with dried gelatin-chitosan hydrogels using a Fourier Transform Infrared (FTIR) Spectrometer (Bruker Vertex 80v, Germany). Each dried gelatin-chitosan hydrogel was placed within the enclosed vacuum chamber one at a time and FTIR spectra were collected within the range of 800–2000 cm^{-1} via attenuated total reflectance (ATR) technique. The measurements were conducted in triplicate and presented in the transmittance mode.

2.4 Rheological Characterization

The rheological properties of PGC hydrogels were evaluated using the Discovery hybrid rheometer (TA instruments, USA). The values of the strain amplitude were first verified to ensure that all measurements were performed within the linear viscoelastic region. Next, the viscosities of PGC hydrogels were evaluated for shear rates ranging from 0.1 to 100 s^{-1} at a constant temperature of 27°C (room temperature). To evaluate the sol-gel transition state of the hydrogels, (i) storage modulus (G') and (ii) loss modulus (G") of the 2.5%, 5% and 7.5% PGC were then measured at varying temperatures from 20 to 40°C at a fixed shear strain of 2%. The sol-gel transition state can be determined by the G'/G" ratio, whereby G'/G" = 1 is the gelling point. All measurements were conducted in triplicate.

2.5 Bioprinting of Biomaterials

A 3-D bioprinter, Biofactory® (regenHU Ltd., Switzerland), was used for printing of PGC hydrogels. The PGC bio-ink was loaded into a sterile printing cartridge and the printing process was conducted using an extrusion-based print-head. The hydrogel was deposited via extrusion-based printing approach and the material flow for each print-head was controlled by individual pressure regulators. Pre-defined structures were input into BioCAD (regenHU Ltd., Switzerland).

The printability of different PGC hydrogels was evaluated using a combination of different printing pressures (1–3.5 bars) and feed rates (600–1000 mm/min) using a constant nozzle diameter of 210 µm. Adjacent filaments of 2 cm length at inter-spacing of 1 mm (n = 6) were printed and measured in terms of filament

widths at varying printing pressures and feed rates using ImageJ processing software. To demonstrate its ability to fabricate a multi-layered hydrogel construct, a 3-layered hydrogel construct with grid-like patterns was fabricated by printing each layer of grid-like patterns directly over the previous layer using an optimal combination of feed rates and printing pressures.

2.6 Biocompatibility of PGC Hydrogels

To assess the biocompatibility of PGC hydrogels, PGC hydrogels were manually casted followed by seeding 150,000 HFF-1 cells on surface of PGC hydrogels in each of the 6-well plates (n = 5) and 2 mL of complete growth medium was added into each well plate. A control setup with 2.5% chitosan was used in this study. The cells were incubated for 4 days prior to performing cell viability assay on Day 4 using Molecular Probes® Live/Dead staining kits (Life-Technologies) according to the manufacturer's manual. The calcein AM will stain the viable cells green, while the ethidium homodimer-1 will stain the dead cells red. The samples were washed twice with PBS and 1 mL of staining solution was added to each of the 6-well plates containing the PGC hydrogels and incubated for an hour before observation under Carl Zeiss Axio Vert. A1 Inverted Microscopy.

3. Results and Discussion

An ideal printable material should provide good shape fidelity and high printing resolution. An important characteristic of printable biomaterials is to have consistent flow that facilitates deposition at high repeatability. Notably, the hydrogel-based bio-inks with natural porosity offer good permeability to oxygen and nutrients[35].

3.1 FTIR Characterization

To evaluate the interactions between the chitosan and gelatin within the polymer blend, FTIR analysis was conducted. The IR spectra of the gelatin-chitosan polymer blend and their respective polymers were shown in Figure 1. The IR spectrum of chitosan polymer displayed saccharide peaks at approximately 896 and 1152 cm^{-1}, an amino characteristic peak at 1550 cm^{-1} and an amide I peak of the acetyl group at 1643 cm^{-1}. Gelatin polymer was characterized by its amino peak at 1539 cm^{-1} and carbonyl peak at 1628 cm^{-1}. The gelatin-chitosan polymer blend led to slight adjustment in the spectrum, i.e., shifting of both carbonyl

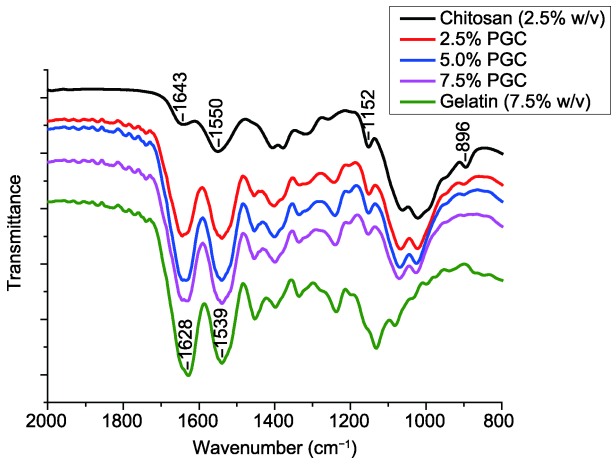

Figure 1. IR spectra of gelatin-chitosan polymer blend along with their individual polymers. The shifting of both carbonyl and amino bands indicate the formation of hydrogen bonds between chitosan and gelatin molecules in the polyelectrolyte complex.

(from 1643 to 1628 cm^{-1}) and amino bands (from 1550 to 1539 cm^{-1}). This illustrated that hydrogen bonding are formed between chitosan and gelatin molecules in the polyelectrolyte complex, which is supported by other reported results[36]. The shifting of the peaks implied that hydrogen bonding occurs between the chitosan and gelatin polymers to form polyelectrolyte hydrogels, which is consistent with previous reported results[30,36,37].

3.2 Rheological Characterization

The rheological properties of different PGC hydrogels were investigated at 27°C to analyze how varying shear rates affect viscosity of the hydrogels during printing process at room temperature. A force is required to overcome yield stress of the hydrogel before it undergoes a shear-thinning process with increasing shear rates. It was reported that a suitable range of printing viscosity is ~ 4 to 30 Pa·s for extrusion-based printing[38]. The generated shear rate in our printing process was estimated in the range of 20–60 s^{-1}. As shown in Figure 2, PGC hydrogels with higher gelatin concentrations exhibited higher yield stress and viscosity. The increased gelatin concentration resulted in more interactions between the positively-charged ammonium ions from chitosan and negatively-charged carboxylate groups from the ampholytic gelatin, resulting in higher viscosity. It was observed that as the shear rate increases, viscosity of 2.5% PGC hydrogels falls out of the ideal printing viscosity. The resultant low viscosity would result in poor printing accuracy

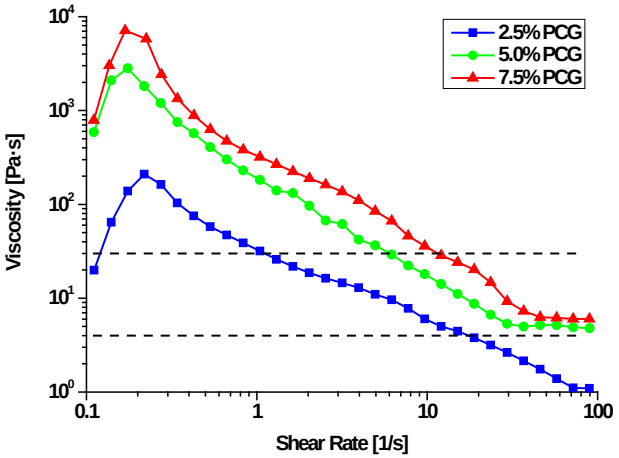

Figure 2. Rheological behavior of PGC hydrogels at varying shear rates (0.1–100 s^{-1}) at 27°C (room temperature). All 3 different PGC hydrogels fall within the suitable range of printing viscosity (~ 4 to 30 Pa·s) at varying shear rates.

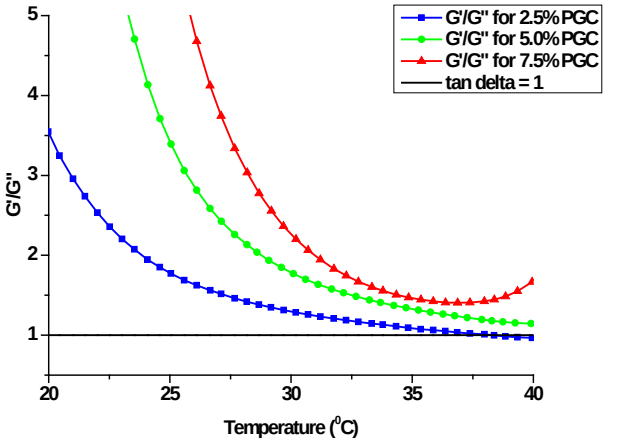

Figure 3. G'/G" ratio of different PGC hydrogels at varying temperatures at fixed shear strain of 2%. A high G'/G" ratio (>1) would offer good shape fidelity of the printed structures.

but both 5% and 7.5% PGC hydrogels have relatively more suitable printing viscosities.

As gelatin is a thermo-sensitive polymer, it is important to evaluate the rheological behaviour of PGC hydrogels at varying temperatures. The storage and loss modulus of PGC hydrogels were evaluated over a temperature range of 20–40°C. Prior to the addition of NaOH, all the PGC hydrogels were in sol state with low viscosity at temperatures above 25°C, as such it is difficult to achieve good shape fidelity above printing temperatures of 25°C. To analyze sol-gel transition state of the PGC hydrogels, the storage (G') and loss modulus (G") of the PGC hydrogels were measured. The ratio of G'/G" (tan α) determines the sol-gel state of the hydrogel. When tan α is greater than 1, it indicates that the material is in a gel state, while a tan α lower than 1 indicates that the material is in a sol state. As shown in Figure 3; only 5% and 7.5% PGC hydrogels exhibit gel-like behaviour within the temperature range of 20–40°C. The tan α of 2.5% PGC hydrogel approaches 1 near 37°C and its tanα value decreases below 1 at temperatures above 37°C. As such, 2.5% PGC hydrogel will not be used in the bioprinting process as loss of shape fidelity might occur during the incubation of the printed construct at higher temperature. Conversely, both 5% and 7.5% PGC hydrogels exhibit significantly high G'/G" ratio, which would offer good shape fidelity of the printed structures.

3.3 Bioprinting of Biomaterials

There are currently two different modes of printing; one is the deposition of cell-laden hydrogel and the other approach is to print the hydrogel and cells separately. The latter approach offers better control over the cellular density and distribution across each printed layer. As such in our printing process, we focus on the printing of acellular biomaterials using the extrusion-based printing technique.

As shown in Figure 4, the suitable range of printing pressures for each PGC hydrogel is different. Generally, higher pressures are required to extrude the more viscous hydrogels[39]. It was observed that the filament widths of 2.5% PGC hydrogels increase exponentially with increasing printing pressures. This is probably due to the intrinsic low viscosity of 2.5% PGC hydrogel which causes higher extent of filament spreading when a larger printing pressure was used. A similar trend was also observed in 5% PGC hydrogel; the filament widths increase in a linear manner from printing pressures of 2–2.8 bars and subsequently increase in an exponential manner when the printing pressures are above 2.8 bars. In contrast, the most viscous 7.5% PGC hydrogels demonstrated a linear relationship between printing pressures and filament widths throughout 2.6 bars to 3.4 bars. It is likely that the high viscosity of 7.5% PGC hydrogel reduces the extent of filament spreading at higher printing pressures (above 3 bars). It was also observed that standard deviation of printed filament widths decreases with PGC hydrogels of higher viscosity. Hence, a more viscous hydrogel offers higher printing consistency and better control over the printed filament widths at increasing printing pressure.

Generally, a higher feed rate would result in a thinner

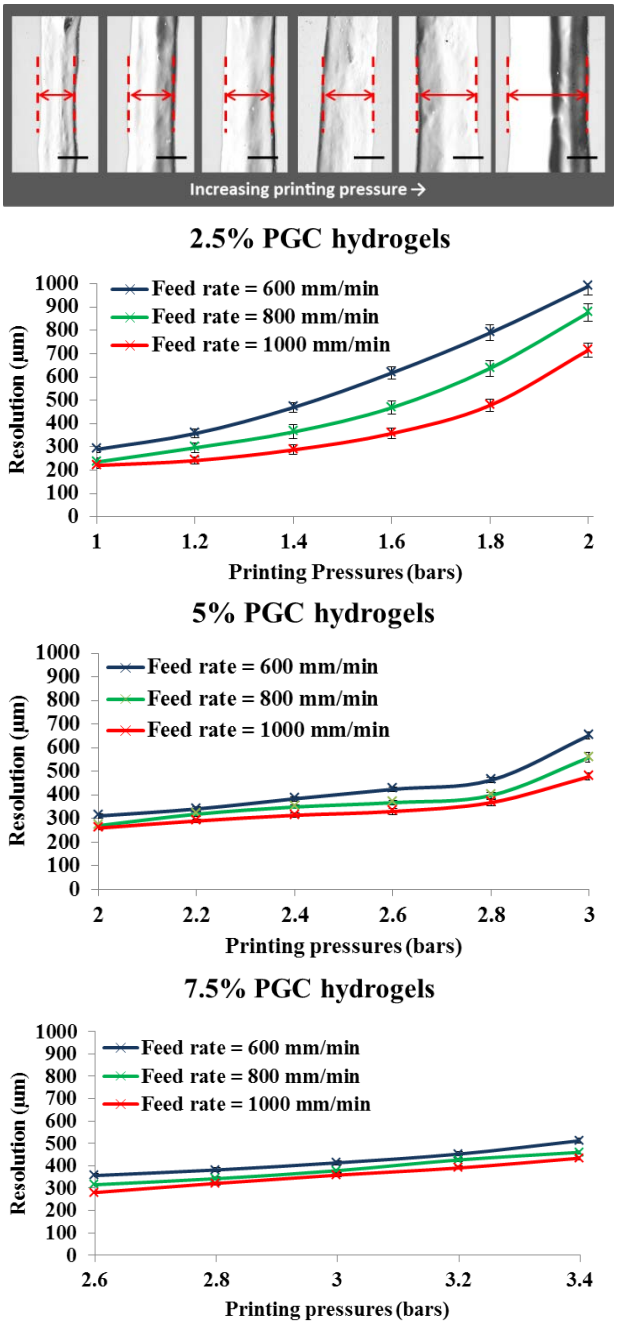

Figure 4. Effect of printing pressures on printed filament widths.

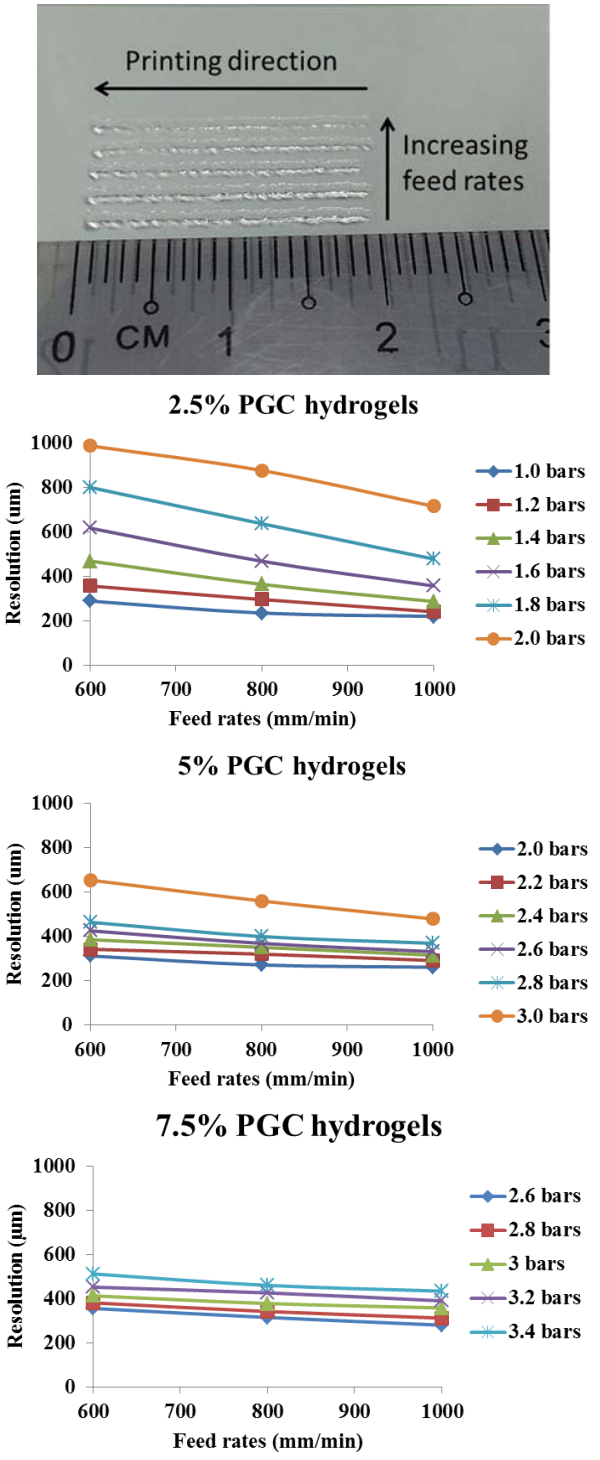

Figure 5. Effect of feed rates on printed filament widths.

filament width (Figure 5). It was observed in 2.5% PGC hydrogels that the printed filament widths increase to a larger extent with decreasing feed rates when higher printing pressures were used (indicated by the gradient of the plotted lines). Conversely, the most viscous 7.5% PGC hydrogels exhibited a linear relationship between the feed rates and printed filament widths within its suitable range of printing pressures. Hence, varying feed rates has significant effect on the less viscous hydrogels such as 2.5% PGC hydrogels with increasing printing pressures.

As shown in Figure 6, an optimal combination of both printing pressures and feed rates is required to obtain a complete grid-like pattern. A high printing pressure would result in excessive material deposition,

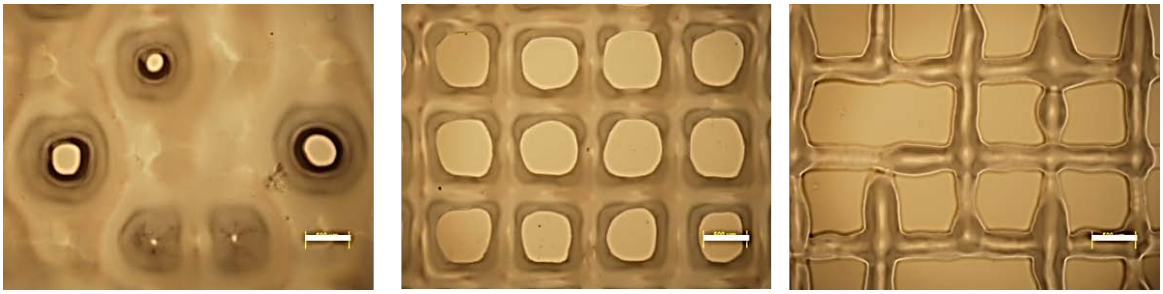

Figure. 6. (Left) Excessive material deposition, (Middle) optimal printing parameters, (Right) incomplete printing (scale bar: 500 µm).

while a low printing pressure would result in incomplete patterning. Among all the PGC hydrogels and different combinations of printing pressures and feed rates, the 5% PGC hydrogels at printing conditions of 2.4 bars and 1000 mm/min feed rate enables the fabrication of complete grid-like patterns at highest printing resolution. Using the optimal combination of printing pressures and feed rates and a pre-defined layer thickness of 160 µm, a 3-layered PGC hydrogel construct with grid-like structures was printed and shown in Figure 7. It was observed that the estimated height of the printed construct (~400 µm) was lower than the pre-defined height of 480 µm and the filament widths increased from ~314 µm (1-layer) to ~ 450 µm (3-layers). It is likely that the nozzle tip transversed within the layer and induced compression of each printed layer (lower height and higher filament widths). Further optimization to the layer thickness is required to improve the accuracy of printed 3D constructs.

3.4 Biocompatibility of PGC Hydrogels

To evaluate the biocompatibility of the PGC hydrogel, 5% PGC hydrogel was manually casted onto 6 well plates followed by seeding of HFF-1 cells onto the surface and a control set-up with 2.5% chitosan was used in this study. The seeded HFF-1 cells were generally round in shape and evenly distributed over the surface of PGC hydrogels. Live-dead staining was conducted to visually inspect the cell viability and morphology after 4 days. As shown in Figure 8, the green viable fibroblast cells exhibited the spindle-like morphology indicating that they were able to attach and proliferate. It was noted that a small number of dead HFF-1 cells, as represented by red colour, was also present in the 3D construct. A greater number of viable HFF-1 cells were observed on 5% PGC hydrogel as compared to the 2.5% chitosan hydrogel. The incorporation of gelatin within the polymer blend improved the biocompatibility by shielding the excessive positive charges on chitosan polymer to a suitable charge density[30]. This enables the cells to attach and proliferate better as compared to the pure chitosan biomaterial[40].

4. Conclusion

We envision that the bioprinting of both biomaterials and cells with pre-defined structures will eventually

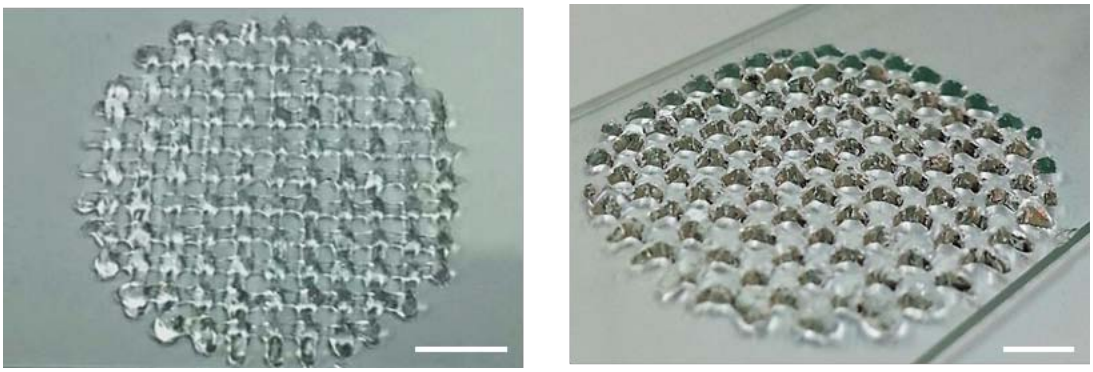

Figure 7. 3D printed multi-layered PGC hydrogel structure view at various persepectives. The resultant 3D construct has a lower height than the pre-defined value and the filament widths increased with increasing layers. 5% PGC hydrogel was tested for the fabrication of 3D hydrogel construct, number of layers 3, scale bar = 5 mm

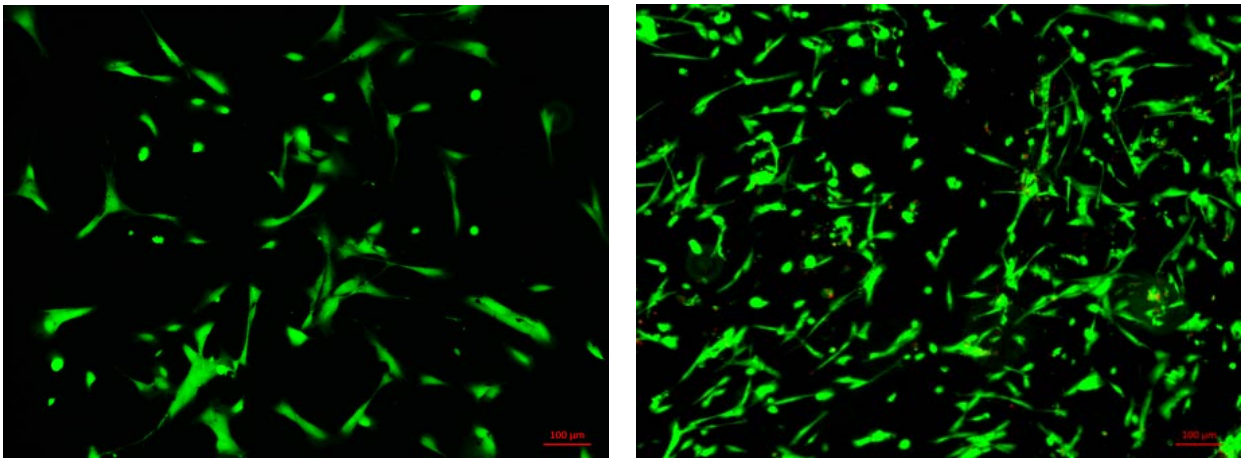

Figure 8. Live-dead staining on Day 4. (Left) chitosan hydrogel, (Right) 5% PGC hydrogel (scale bar: 100 μm).

mature to form a functional tissue. As such, 3D bioprinting serves as an attractive platform to facilitate cellular and matrix deposition in a spatially-controlled 3D matrix. Chitosan is a promising polymer used in wound healing applications due to its antimicrobial and hemostasis properties. In this work, modification to the chitosan was carried out via the addition of gelatin to form printable polyelectrolyte gelatin-chitosan (PGC) hydrogels. We have optimized PGC hydrogels for bioprinting of skin constructs. The PGC hydrogels exhibited a sufficiently high viscosity that is suitable for our printing chamber which has a temperature of 27°C and its high G'/G" ratio resulted in good shape fidelity of the printed constructs. The highest resolution for the grid-like pattern using the 210 μm nozzle tip was 314 μm at an optimal combination of 2.4 bars and 1000 mm/min feed rate. The important functions of bioengineered skin are to provide barrier function and a temporary scaffold to guide tissue morphogenesis[41]. The use of bioprinting offers good spatial control over deposition of selected biomaterials at specific regions to fabricate customizable tissue-engineered constructs correlating to wound area and depth. Full-thickness human skin ranges between 1.5–2.5 mm in thickness. The epidermal region is approximately 75 to 150 μm in thickness and the dermal region is usually less than 2 mm. The printed constructs (~400 μm for 3 layers) are representative of the outer epidermal layer and part of the dermal region. These results suggest the potential use of PGC hydrogels for bioprinting applications. More work needs to be conducted on thixotropy and swelling behavior of the PCG hydrogels to further optimize the printing process.

Conflict of Interest and Funding

No conflict of interest was reported by the authors.

Acknowledgments

The first author would like to thank the scholarship sponsorship by A*STAR Graduate Academy.

References

1. Lanza R, Langer R and Vacanti J P, 2011, *Principles of Tissue Engineering*, 4th edn, Academic Press, San Diego.
2. Watt F M and Fujiwara H, 2011, Cell-extracellular matrix interactions in normal and diseased skin. *Cold Spring Harbor Perspectives in Biology*, vol.3(4): a005124. http://dx.doi.org/10.1101/cshperspect.a005124
3. Murphy S V and Atala A, 2014, 3D bioprinting of tissues and organs, *Nature biotechnology*, vol.32: 773–785. http://dx.doi.org/10.1038/nbt.2958
4. Ozbolat I T and Yu Y, 2013, Bioprinting towards organ fabrication: Challenges and future trends. *IEEE Transactions on Bio-Medical Engineering*, vol.60(3): 691–693. http://dx.doi.org/10.1109/TBME.2013.2243912
5. Lee V, Singh G, Trasatti C, *et al.*, 2013, Design and fabrication of human skin by three-dimensional bioprinting. *Tissue Engineering Part C: Methods*, vol.20(6): 473–484. http://dx.doi.org/10.1089/ten.TEC.2013.0335
6. Koch L, Deiwick A, Schlie S, *et al*., 2012, Skin tissue generation by laser cell printing. *Biotechnology and Bioengineering*, vol.109(7): 1855–1863. http://dx.doi.org/10.1002/bit.24455
7. Pereira R F, Barrias C C, Granja P L, *et al.*, 2013, Advanced biofabrication strategies for skin regeneration and repair. *Nanomedicine*, vol.8(4): 603–621.

http://dx.doi.org/10.2217/nnm.13.50

8. Cui X, Breitenkamp K, Finn M, *et al*., 2012, Direct human cartilage repair using three-dimensional bioprinting technology. *Tissue Engineering Part A*, vol.18(11-12): 1304–1312. http://dx.doi.org/10.1089/ten.tea.2011.0543
9. Kundu J, Shim J H, Jang J, *et al.*, 2013, An additive manufacturing-based PCL alginate-chondrocyte bioprinted scaffold for cartilage tissue engineering. *Journal of Tissue Engineering and Regenerative Medicine*, vol.9(11): 1286–1297. http://dx.doi.org/10.1002/term.1682
10. Chang R, Emami K, Wu H, *et al*., 2010, Biofabrication of a three-dimensional liver micro-organ as an *in vitro* drug metabolism model. *Biofabrication*, vol.2(4): 045004. http://dx.doi.org/10.1088/1758-5082/2/4/045004
11. Binder K W, Zhao W X, Aboushwareb T, *et al*., 2010, *In situ* bioprinting of the skin for burns. *Journal of the American College of Surgeons*, vol.211(3): S76. http://dx.doi.org/10.1016/j.jamcollsurg.2010.06.198
12. Tobin D J, 2006, Biochemistry of human skin—our brain on the outside. *Chemical Society Reviews*, vol.35(1): 52–67. http://dx.doi.org/10.1039/B505793K
13. Ng W L, Yeong W Y and Naing M W, 2015, Cellular approaches to tissue-engineering of skin: A review. *Journal of Tissue Science & Engineering*, vol.6: 150. http://dx.doi.org/10.4172/2157-7552.1000150
14. Michael S, Sorg H, Peck C-T, *et al.*, 2013, Tissue engineered skin substitutes created by laser-assisted bioprinting form skin-like structures in the dorsal skin fold chamber in mice. *Plos One*, vol.8: e57741. http://dx.doi.org/10.1371/journal.pone.0057741
15. Lee W, Debasitis J C, Lee V K, *et al.*, 2009, Multi-layered culture of human skin fibroblasts and keratinocytes through three-dimensional freeform fabrication. *Biomaterials*, vol.30(8): 1587–1595. http://dx.doi.org/10.1016/j.biomaterials.2008.12.009
16. Lee W, Lee V, Polio S, *et al.*, 2010, On-demand three-dimensional freeform fabrication of multi-layered hydrogel scaffold with fluidic channels. *Biotechnology and Bioengineering*, vol.105(6): 1178–1186. http://dx.doi.org/10.1002/bit.22613
17. Weber L, Kirsch E, Müller P, *et al.*, 1984, Collagen type distribution and macromolecular organization of connective tissue in different layers of human skin. *Journal of Investigative Dermatology*, vol.82(2): 156–160. http://dx.doi.org/10.1111/1523-1747.ep12259720
18. Muzzarelli R A, 2009, Chitins and chitosans for the repair of wounded skin, nerve, cartilage and bone. *Carbohydrate Polymers*, vol.76(2): 167–182. http://dx.doi.org/10.1016/j.carbpol.2008.11.002
19. Dash M, Chiellini F, Ottenbrite R M, *et al*., 2011, Chitosan—A versatile semi-synthetic polymer in biomedical applications. *Progress in Polymer Science*, vol.36(8): 981–1014. http://dx.doi.org/10.1016/j.progpolymsci.2011.02.001
20. Jayakumar R, Prabaharan M, Kumar P S, *et al.* 2011, Biomaterials based on chitin and chitosan in wound dressing applications. *Biotechnology Advances*, vol.29(3): 322–337. http://dx.doi.org/10.1016/j.biotechadv.2011.01.005
21. Rinaudo M, 2006, Chitin and chitosan: Properties and applications. *Progress in Polymer Science*, vol.31(7): 603–632. http://dx.doi.org/10.1016/j.progpolymsci.2006.06.001
22. Kim I Y, Seo S J, Moon H S, *et al.*, 2008, Chitosan and its derivatives for tissue engineering applications. *Biotechnology Advances*, vol.26(1): 1–21. http://dx.doi.org/10.1016/j.biotechadv.2007.07.009
23. Ueno H, Nakamura F, Murakami M, *et al.*, 2001, Evaluation effects of chitosan for the extracellular matrix production by fibroblasts and the growth factors production by macrophages. *Biomaterial*s, vol.22(15): 2125–2130. http://dx.doi.org/10.1016/S0142-9612(00)00401-4
24. Kong M, Chen X G, Xing K, *et al.*, 2010, Antimicrobial properties of chitosan and mode of action: A state of the art review. *International Journal of Food Microbiology*, vol.144(1): 51–63. http://dx.doi.org/10.1016/j.ijfoodmicro.2010.09.012
25. Cho Y-W, Jang J, Park C R, *et al.*, 2000, Preparation and solubility in acid and water of partially deacetylated chitins. *Biomacromolecules*, vol.1(4): 609–614. http://dx.doi.org/10.1021/bm000036j
26. Geng L, Feng W, Hutmacher D W, *et al*., 2005, Direct writing of chitosan scaffolds using a robotic system. *Rapid Prototyping Journal*, vol.11(2): 90–97. http://dx.doi.org/10.1108/13552540510589458
27. Ng W L, Yeong W Y and Naing M W, 2014, Potential of bioprinted films for skin tissue engineering, in *Proceedings of the 1st International Conference on Progress in Additive Manufacturing* (eds C K Chua, W Y Yeong, M J Tan and E Liu).
28. Malafaya P B, Silva G A and Reis R L, 2007, Natural–origin polymers as carriers and scaffolds for biomolecules and cell delivery in tissue engineering applications. *Advanced Drug Delivery Reviews*, vol.59(4–5): 207–233. http://dx.doi.org/10.1016/j.addr.2007.03.012
29. Huang Y, Onyeri S, Siewe M, *et al.*, 2005, *In vitro* characterization of chitosan–gelatin scaffolds for tissue engineering. *Biomaterials*, vol.26(36): 7616–7627. http://dx.doi.org/10.1016/j.biomaterials.2005.05.036

30. Yin Y, Li Z, Sun Y, *et al*., 2005, A preliminary study on chitosan/gelatin polyelectrolyte complex formation. *Journal of Materials Science*, vol.40(17): 4649–4652. http://dx.doi.org/10.1007/s10853-005-3929-9
31. Mao J, Zhao L G, Yin Y J, *et al*., 2003, Structure and properties of bilayer chitosan–gelatin scaffolds. *Biomaterials*, vol.24(6): 1067–1074. http://dx.doi.org/10.1016/S0142-9612(02)00442-8
32. Mao J , Zhao L, de Yao K, *et al*., 2003, Study of novel chitosan-gelatin artificial skin *in vitro*. *Journal of Biomedical Materials Research Part A*, vol.64A(2): 301–308. http://dx.doi.org/10.1002/jbm.a.10223
33. Pereda M, Ponce A, Marcovich N, *et al.*, 2011, Chitosan-gelatin composites and bi-layer films with potential antimicrobial activity. *Food Hydrocolloids*, vol.25(5): 1372–1381. http://dx.doi.org/10.1016/j.foodhyd.2011.01.001
34. Wang X, Yu X, Yan Y, *et al.*, 2008, Liver tissue responses to gelatin and gelatin/chitosan gels. *Journal of Biomedical Materials Research Part A*, vol.87(1): 62–68. http://dx.doi.org/10.1002/jbm.a.31712
35. Nguyen K T and West J L, 2002, Photopolymerizable hydrogels for tissue engineering applications. *Biomaterials*, vol.23(22): 4307–4314. http://dx.doi.org/10.1016/S0142-9612(02)00175-8
36. Cheng M, Deng J, Yang F, *et al.*, 2003, Study on physical properties and nerve cell affinity of composite films from chitosan and gelatin solutions. *Biomaterials*, vol.24(17): 2871–2880. http://dx.doi.org/10.1016/S0142-9612(03)00117-0
37. Yin Y J, Yao K D, Cheng G X, *et al*., 1999, Properties of polyelectrolyte complex films of chitosan and gelatin. *Polymer International*, vol.48(6): 429–432. http://dx.doi.org/10.1002/(SICI)1097-0126(199906)48:6<429::AID-PI160>3.0.CO;2-1
38. Das S, Pati F, Choi Y J, *et al*., 2015, Bioprintable, cell-laden silk fibroin–gelatin hydrogel supporting multilineage differentiation of stem cells for fabrication of three-dimensional tissue constructs. *Acta Biomaterialia*, vol.11: 233–246. http://dx.doi.org/10.1016/j.actbio.2014.09.023
39. Swope V B, Supp A P and Boyce S T, 2002, Regulation of cutaneous pigmentation by titration of human melanocytes in cultured skin substitutes grafted to athymic mice. *Wound Repair and Regeneration*, vol.10(6): 378–386. http://dx.doi.org/10.1046/j.1524-475X.2002.10607.x
40. Mao J S, Cui Y L, Wang X H, *et al.* 2004, A preliminary study on chitosan and gelatin polyelectrolyte complex cytocompatibility by cell cycle and apoptosis analysis. *Biomaterials*, vol.25(18): 3973–3981. http://dx.doi.org/10.1016/j.biomaterials.2003.10.080
41. MacNeil S, 2007, Progress and opportunities for tissue-engineered skin. *Nature*, vol.445: 874–880. http://dx.doi.org/10.1038/nature05664